HHS Public Access

Author manuscript

Mol Cancer Res. Author manuscript; available in PMC 2016 June 01.

Published in final edited form as:

Mol Cancer Res. 2015 June ; 13(6): 957–968. doi:10.1158/1541-7786.MCR-14-0580.

A YAP/TAZ-Regulated Molecular Signature is Associated with Oral Squamous Cell Carcinoma

Samantha E. Hiemer[1], **Liye Zhang**[2,*], **Vinay K. Kartha**[2,*], **Trevor S. Packer**[3], **Munirah Almershed**[3], **Vikki Noonan**[4], **Maria Kukuruzinska**[3], **Manish V. Bais**[3], **Stefano Monti**[2], and **Xaralabos Varelas**[1]

[1]Department of Biochemistry, Boston University School of Medicine

[2]Section of Computational Biomedicine, Boston University School of Medicine

[3]Department of Molecular and Cell Biology, Boston University School of Dental Medicine

[4]Division of Oral Pathology, Boston University School of Dental Medicine

Abstract

Oral squamous cell carcinoma (OSCC) is a prevalent form of cancer that develops from the epithelium of the oral cavity. OSCC is on the rise worldwide, and death rates associated with the disease are particularly high. Despite progress in understanding of the mutational and expression landscape associated with OSCC, advances in deciphering these alterations for the development of therapeutic strategies have been limited. Further insight into the molecular cues that contribute to OSCC is therefore required. Here we show that the transcriptional regulators YAP (*YAP1*) and TAZ (*WWTR1*), which are key effectors of the Hippo pathway, drive pro-tumorigenic signals in OSCC. Regions of pre-malignant oral tissues exhibit aberrant nuclear YAP accumulation, suggesting that dysregulated YAP activity contributes to the onset of OSCC. Supporting this premise, we determined that nuclear YAP and TAZ activity drives OSCC cell proliferation, survival, and migration *in vitro*, and is required for OSCC tumor growth and metastasis *in vivo*. Global gene expression profiles associated with YAP and TAZ knockdown revealed changes in the control of gene expression implicated in pro-tumorigenic signaling, including those required for cell cycle progression and survival. Notably, the transcriptional signature regulated by YAP and TAZ significantly correlates with gene expression changes occurring in human OSCCs identified by “The Cancer Genome Atlas” (TCGA), emphasizing a central role for YAP and TAZ in OSCC biology.

Introduction

Oral squamous cell carcinoma (OSCC) originates from the epithelium of the oral cavity and represents the majority of head and neck cancers. Very poor survival rates are associated with those afflicted by OSCC (only ~50% survival over five-years), and unfortunately little

Corresponding author: Xaralabos Varelas, PhD, Boston University School of Medicine, 72 East Concord Street, Room K225, Boston, MA 02118, Phone: 617-638-4182, Fax: 617-638-5339, xvarelas@bu.edu.

*These authors contributed equally

The authors have no conflict of interest to disclose

progress has been made with treatment strategies over the past few decades (1). Therefore, understanding dysregulated molecular cues associated with OSCC onset and progression is an important step in the development of effective therapeutics.

Recent studies have shown that aberrant activation of the transcriptional regulators YAP and TAZ (YAP/TAZ) contributes to the onset and progression of a range of cancers (2). YAP/TAZ transcriptional activity is dependent on their recruitment to the nucleus, which promotes binding to a range of transcription factors, most notably the TEAD family (3, 4). YAP/TAZ-directed transcription promotes cell proliferation, pro-survival, and cell migration signals, all of which contribute to the pro-tumorigenic roles of YAP/TAZ (5–7). Multiple signaling events restrict YAP/TAZ from the nucleus, the best characterized of which are signals mediated by the Hippo pathway (8). In particular, Hippo pathway activation promotes the phosphorylation of YAP and TAZ on conserved serine residues that lead to sequestration and destabilization of YAP/TAZ in the cytoplasm (7, 9, 10). Mechanical cues and signals that affect cytoskeletal dynamics, such as those transduced by G-protein-coupled receptors (GPCRs), also control YAP/TAZ localization, both by regulating Hippo pathway activity and via Hippo pathway-independent cues (11). While the signals regulating YAP/TAZ localization are not completely understood, recent work indicates is that precise control of these signals are required to maintain tissue homeostasis (12).

Dysregulated YAP/TAZ activity has been implicated in head and neck cancers. For example, YAP expression has been shown to correlate with poor patient survival in head and neck cancers (13, 14), and increased YAP levels and nuclear localization are associated with high-grade OSCC (14, 15). TAZ overexpression has also been shown to be significantly associated with head and neck tumor size, histopathological grade, and reduced patient survival (14). Furthermore, elevated nuclear YAP/TAZ levels are known to promote resistance to several cancer treatments, including those commonly used for OSCC therapy, such as cisplatin and cetuximab (16–18). While evidence supports a role for YAP/TAZ in OSCCs, little is known about the downstream events regulated by YAP/TAZ, and at what step in cancerogenesis these factors may be involved.

Given the potential importance of TAZ and/or YAP signaling, we sought to gain a better understanding of their roles in OSCC. To this end, we integrated the use of patient tissue samples, functional assays *in vitro* and *in vivo*, genome-wide expression profiling, and analyses of publically available expression data from studies performed by “The Cancer Genome Atlas” (TCGA) groups. Our observations have revealed that YAP localization is dysregulated in benign and early pre-malignant oral tissues, and that elevated YAP protein levels are evident in a subset of OSCCs. Further, we show that nuclear YAP and TAZ activity drive pro-tumorigenic signals in OSCC cells *in vitro*, and that YAP and TAZ are necessary for OSCC development and metastasis *in vivo*. A global analysis of YAP/TAZ-regulated gene expression exposed a transcriptional program associated with expression changes found in OSCC onset and progression. Our data therefore highlight novel YAP/TAZ-regulated events in OSCC, and offer an important gene expression signature that may serve as a resource for OSCC detection and personalized therapeutic development strategies.

Materials and Methods

Human oral tissue specimens

Tissue specimens were obtained from patients at Boston University Medical Center, and were acquired from scalpel-generated incisional biopsies of oral epithelium (benign epithelial hyperplasia (n=7), mild (n=3) and severe (n=3) dysplasia), as well as from surgical resections of moderately differentiated (n=6) and poorly differentiated (n=4) OSCCs of the lateral tongue border and of the floor of the mouth. For each condition, cytologically normal adjacent epithelia were also obtained and analyzed. Benign epithelial hyperplasia, dysplasia, and OSCC regions, as well as adjacent epithelia, were defined by an on-site histopathological examination and tissues were snap-frozen at −80°C. A portion of the tissues were sectioned and used for hematoxylin and eosin (H&E) staining and immunofluorescence imaging. Sections (3 μm) of tissues were placed on OptiPlus Positive-Charged Barrier Slides (BioGenex), deparaffinized, treated with Retrievit-6 Target Retrieval Solution (BioGenex), and then processed. OSCC tissues were lysed for biochemical analysis (see below). The institutional review board (IRB) at the Boston University Medical Campus approved the use of human oral tissue specimens for our studies.

Cell culture, plasmids, and transfections

Tested and authenticated CAL27, SCC9, SCC15 and SCC25 cells were purchased from ATCC. UM-SCC2 cells (herein referred to as SCC2 cells) were a kind gift from Roberto Weigert (NIH), and were described previously (19). CAL27 and SCC2 cells were cultured in DMEM supplemented with 10% FBS. SCC9, SCC15 and SCC25 cells were cultured in DMEM/F12 media (1:1) supplemented with 400 ng/mL hydrocortisone (Sigma) and 10% FBS. CAL27 doxycycline-inducible stable cell lines were generated using the lentiviral Tet-On system (Clontech). 3xFLAG-tagged mutants of YAP (5SA: S61A, S109A, S127A, S164A, S97A or 5SA/S94A) were generated by site-directed mutagenesis and cloned into the pLVX-Tight-Puro plasmid (#632162, Clontech). CAL27 stable cells were selected with 1 mg/mL G-418 sulfate (Gold Biotechnology) and 1 μg/mL Puromycin (Invivogen). RNA interference was performed by transfecting siRNA using Dharmafect 1 (Thermo Scientific) according to manufacturer's protocol. Lentiviral transduction of CMV-promoter driven dsRED was used to generate SCC2-dsRED cells. SCC2-dsRED cells were subsequently infected with lentivirus transducing the expression of control shRNA (shCTL), shRNA targeting YAP (shYAP-2, pLKO1-shYAP-2 was a gift from Kunliang Guan, Addgene plasmid # 27369 (4)) and/or TAZ (shTAZ (20)) from either the pLKO1-puro (gift from Bob Weinberg (21)) or pLKO1-neo plasmids (gift from Sheila Stewart). The following SCC2-dsRED stable cells were generated and selected with 2 mg/mL G-418 sulfate and 1 μg/mL Puromycin: Neo-shCTL+Puro-shCTL (shCTL), Neo-shYAP+Puro-shCTL (shYAP), Neo-shYAP+Puro-shTAZ (shY/T). Sequences for the shRNA and siRNA used are outlined in Supplementary Table 1.

Immunoblotting and immunofluorescence microscopy

Oral cancer cells were lysed in 50mM Tris-Cl (pH 7.5), 150mM NaCl, 1mM EDTA, 0.5% Triton X-100, and protease inhibitors, and endogenous protein levels were examined by SDS-PAGE followed by immunoblotting. Tissue lysates were prepared from adjacent

epithelia and OSCC using Triton/β-octylglucoside buffer, as previously described (22). Protein concentrations were determined using BCA assay (Pierce) and equal protein fractions were analyzed by immunoblotting. Quantitation of immunoblot data was performed using Image Lab software (Bio-Rad). Antibodies used for immunoblotting are outlined in Supplementary Table 2.

For the analysis of oral cancer cell lines by immunofluorescence microscopy, cells were fixed with 4% paraformaldehyde, permeabilized with 0.1% Triton X-100-PBS, blocked in 2% BSA-PBS, and probed with primary and secondary antibodies outlined in Supplementary Table 2. Nuclei were stained with Hoechst. Images were captured using a Zeiss LSM 700 confocal microscope and processed using Volocity software (PerkinElmer). For the analysis of human tissue samples, sections were blocked with 10% goat serum and incubated with rabbit-anti-YAP antibody (Abcam; see Supplementary Table 2) followed by a secondary antibody conjugated to Alexa Fluor 555. Sections were counterstained for nuclei with 4′,6-diamidino-2-phenylindole, dihydrochloride (DAPI). Tissues analyzed in the absence of primary antibodies were used as negative controls. The slides were mounted in Vectashield and optical sections (0.5 μm) were analyzed by confocal microscopy using an LSM510 Zeiss Axiovert 200M confocal microscope.

Cell proliferation analysis

SCC2 cells were transfected with scrambled control siRNA, or siRNA targeting TAZ, YAP, or both YAP/TAZ for 24 hours. Cells were plated (5×10^4 cells) (Day 0) and counted each day for 6 consecutive days (Day 1–6), with media changed every 2 days. CAL27 doxycycline-inducible cells were pre-treated with doxycycline (100 ng/mL, Clontech) for 24 hours. Cells were plated (5×10^4 cells) (Day 0) in the presence of doxycycline. Cells were counted every 2 days for 2 weeks (Day 2–14) and media were changed every 2 days.

Caspase 3/7 activity assays

SCC2 cells were transfected with scrambled control siRNA, or siRNA targeting TAZ, YAP, or both YAP/TAZ, and cultured for 48 hours. CAL27 doxycycline-inducible cells were treated with doxycycline (100 ng/mL) for 24 hours to induce the expression of YAP-5SA, or 5SA/S94A. Cleaved Caspase-3 and -7 activity was measured using the Caspase-Glo 3/7 kit (Promega) according to manufacturer's protocol. Statistical analysis was conducted with Prism software (GraphPad) using a two-tailed unpaired Student's *t* test.

Wound healing scratch assays

SCC2 cells were transfected with scrambled control siRNA, or siRNA targeting TAZ, YAP, or both YAP/TAZ, and cultured for 48 hours. CAL27 doxycycline-inducible cells were pretreated with doxycycline (100 ng/mL) for 24 hours to induce the expression of YAP-5SA, or 5SA/S94A. Monolayers were wounded and photographed at 0 hours and after then after additional 12 or 24 hours. Images were captured and analyzed using ImageJ software. Statistical analysis was conducted with Prism software (GraphPad) using a two-tailed unpaired Student's *t* test.

Tongue orthotopic mouse injections and IVIS imaging

All experiments were approved by the Boston University Medical Center IACUC. Two month old female nude mice (NCr nu/nu; Taconic Farms, Hudson, NY) were injected in the tongue with 3×10^5 SCC2-dsRed shCTL, shYAP, or shY/T cells (n=9 mice per group) in respective groups after anesthetizing with 4% isoflurane. Primary tumors were directly measured with calipers on day 10, 15, 18, and 22 to obtain tumor volume. IVIS imaging was performed on day 22 using the Caliper IVIS Spectrum Imaging System (Xenogen) to visualize fluorescence (570 nm excitation, 620 nm emission, exposed for 1.0 second). Regions of interest (ROI) were quantitated for each mouse using Living Image software and background radiant effiency in vehicle mice was subtracted. Statistical analysis was conducted with Prism software (GraphPad) using a two-tailed unpaired Student's *t* test.

Microarrays

SCC2 cells were transfected with control siRNA, or siRNAs targeting TAZ, YAP, or YAP/TAZ. After 48 hours, total RNA from three independent experiments carried out on separate days was isolated and purified by RNeasy Mini Kit (Qiagen), and the samples were then profiled on Affymetrix Human Gene 2.0 Chips at the Boston University Microarray Core. The microarray data is available at Gene Expression Omnibus (GEO); accession GSE66949. The expression profiles were processed and normalized using the Robust Multi-array Average (RMA) procedure (23) based on a custom Brainarray CDF (24). For each of the siRNA experiments, signatures of genes differentially expressed between treatment and corresponding siRNA control with an FDR q-value ≤0.05 and a fold change ≥2 were identified as either *activated* (up-regulated in control) or *repressed* (up-regulated in treatment). The overlap between the differentially expressed gene signatures was evaluated by Fisher test. Hierarchical gene and sample clustering was performed on the top 3000 genes with highest median absolute deviation (MAD; a robust version of the variance) across 12 samples, using "ward" as the agglomeration rule, and 1 minus Pearson correlation and Euclidean as the distance measures for genes and samples, respectively.

Quantitative real time PCR (qPCR)

SCC2 cells were transfected with control siRNA, or siRNA targeting TAZ, YAP, or both YAP/TAZ, and cultured for 48 hours. CAL27 doxycycline-inducible cells were pretreated with doxycycline (100 ng/mL) for 24 hours to induce the expression of control vector, YAP-5SA, or 5SA/S94A. Total RNA was collected and purified using RNeasy mini prep kit (Qiagen). cDNA synthesis was performed using 1 μg RNA and iScript cDNA synthesis kit (Bio-Rad) according to manufacturer's protocol. qPCR was performed using Fast SYBR green enzyme (Applied Biosystems) and measured on ViiA 7 real time PCR system (Applied Biosystems). Transcript levels were analyzed using the ΔΔCT method and normalized to GAPDH. Statistical analysis was conducted with Prism software (GraphPad) using a two-tailed unpaired Student's *t* test. Primer sequences are indicated in Supplementary Table 3.

Expression analysis of the Cancer Genome Atlas (TCGA) OSCC data

Normalized Level 3 gene expression (RNASeqV2) and associated clinical data were obtained from TCGA corresponding to the Head and Neck Squamous Cell Carcinoma (HNSC) dataset (n=340; https://tcga-data.nci.nih.gov/tcga/). Samples were filtered so as to retain only those belonging to one of six oral cancer anatomic subtypes (Alveolar Ridge, Base of tongue, Buccal Mucosa, Floor of mouth, Oral cavity, Oral tongue), and only Caucasian patients were analyzed (filtered Oral Cancer dataset size: n=193). Box plots of the expression values were generated with respect to tumor grade/stage for YAP and TAZ (log2-transformed).

Hierarchical clustering of expression signatures and projection on tumor progression

Caucasian samples from six oral sites (alveolar ridge, base of tongue, buccal mucosa, floor of mouth, oral cavity, and tongue) were used for the hierarchical clustering analysis (n=193), and two clear clusters of YAP/TAZ-activated genes were identified. Each cluster was annotated by pathway enrichment based on a hyper-geometric test against the set of curated pathways (c2.cp) in the MSigDB compendium (25). To test whether gene signatures defined by microarray experiments were up- or down- regulated with respect to tumor status or tumor grade/stage, GSEA analysis was performed to test whether the activated/repressed gene signatures were enriched in tumor versus normal or higher grade versus lower grade tumors (26).

Hyperenrichment analysis

To evaluate whether specific pathways or transcription factors might play a role in the response to targeted inhibition, we carried out enrichment analysis of the differential signatures based on a hyper-geometric test. To this end, each of the up- and down-regulated signatures (with FDR≤0.05 and fold-change≥2) was tested against the MSigDB c2.cp (canonical pathways), c3.all (TF/miR targets), and c6.all (oncogenic pathways) compendiums.

Results

Nuclear YAP accumulation marks pre-malignant dysplastic regions of the oral epithelium

The increased activity of the transcriptional regulator YAP has been implicated in the progression of oral squamous cell carcinoma (OSCC) (14, 15, 27, 28). In particular, increased YAP levels have been associated with OSCC and other head and neck cancers, with subsets of these cancers exhibiting elevated nuclear YAP accumulation (15, 27). Dysregulated nuclear YAP is known to drive overgrowth of several tissues (2), and thus YAP-driven cues may contribute to early events in OSCC development. Since examination of benign and pre-malignant oral epithelial tissues has been limited, we set out to characterize a potential relationship between YAP and the pathology linked to OSCC predisposition. Specifically, we examined a range of tissues characterized as benign epithelial hyperplasia, mild and severe dysplasia, as well as morphologically adjacent epithelium from the oral cavity of human patients. Using immunofluorescence microscopy we observed very low levels of YAP in most cells found in the tissues of adjacent

epithelium, except for YAP residing in the basal cell population, which exhibited relatively high levels in both the nuclear and cytoplasmic compartments (Fig. 1). We observed the emergence of cells marked with prominent nuclear YAP beyond the basal cell population in regions of dysplastic tissues, with highly enriched nuclear YAP in areas with severe dysplasia pathology (Fig. 1, and Supplementary Fig. S1). Interestingly, nuclear YAP was evident even in regions of benign epithelial hyperplasia (Fig. 1, and Supplementary Fig. S1). Our observations therefore suggest that predisposition to OSCC may be related to the dysregulation of YAP localization.

Prior studies have suggested that amplification of the chromosomal region encoding *YAP* contributes to its aberrant expression in human head and neck squamous cell carcinoma cells (27, 29). We therefore examined whether increased *YAP* expression may be linked to OSCC onset, and further characterized the prevalence of this potential dysregulation. For this, we made use of data from a large number of patient samples publically available from TCGA to examine potential *YAP* gene expression, amplification, and/or mutations. We also included *TAZ* in our analysis of the TCGA data. We found no evidence of amplification, deletion, or mutation of the genomic region encompassing *YAP* or *TAZ* in cancers originating from the oral cavity (using the Genomic Identification of Significant Targets in Cancer tool; data not shown). Further, we found that *YAP* (Fig. 2A) and *TAZ* (Fig. 2B) expression was not significantly altered with tumor grade or stage.

Given that expression/mutation analysis may not reflect what is occuring with *YAP* protein levels, we obtained and examined protein from ten fresh OSCC tumors and their respective adjacent epithelia. Four of the tumors exhibited poorly differentiated pathology, and these tumors showed high levels of YAP compared to normal adjacent epithelia (Fig. 2C, and Supplementary Fig. S2A). Phosphorylation of YAP on Serine 127 (pS127-YAP) induces the cytoplasmic sequestration of YAP (7, 30), and correlates with YAP degradation (10). This post-translational modification was relatively low in the poorly differentiated tumors (Fig. 2C), providing a potential explanation for the observed elevated YAP protein levels. The other six tumors we examined, which were characterized as moderately differentiated, showed no differences in YAP or pS127-YAP (Fig. 2C, and Supplementary Fig. S2B). Our data therefore suggest that dysregulated hypo-phosphorylated YAP might contribute to the distinct pathology of a subset of OSCCs.

YAP/TAZ promote tumorigenic phenotypes in OSCC cells

To gain further insight into the contributions of YAP to OSCC development we utilized available OSCC cell lines to carry out functional assays following repressed or induced YAP activity. We started by examining YAP and pS127-YAP levels in lysates obtained from a panel of OSCC cell lines with different tumorigenic capacities: CAL27, SCC2, SCC9, SCC15, and SCC25 cells. We found that YAP levels were highest in the SCC2, which are cells that have aggressive metastatic properties in mouse xenograft models (19). YAP in the SCC2 cells was also hypo-phosphorylated on S127 as compared to the other cells (Fig. 3A). The relative differences in pS127-YAP were reflected in the compaction-induced sequestration of YAP into the cytoplasm of these cells, an event associated with contact-mediated proliferation arrest (31) (Fig. 3B). In particular, nuclear YAP levels in the SCC2

cells were not altered in response to cell compaction (Fig. 3B). Thus, our observations suggest that increased hypo-phosphorylated nuclear YAP may relate to the aggressive behavior of SCC2 cells.

Prior studies have indicated important roles for YAP and TAZ in the control of cell proliferation and survival (2). To test YAP activity in OSCC cells we decided to use the SCC2 and CAL27 cells as models for high and low nuclear YAP activity, respectively. First, SCC2 cells were transfected with siRNA to deplete YAP levels, and since TAZ might have complimentary roles, we also depleted TAZ, or both YAP/TAZ levels (Fig. 4A). Analyses of cell numbers over time indicated that the knockdown of YAP, TAZ, or both YAP/TAZ decreased the ability of SCC2 cells to proliferate, with YAP knockdown affecting the cells more than TAZ knockdown, but YAP/TAZ knockdown having the most pronounced effect (Fig. 4B). Examination of SCC2 cells that were depleted of YAP/TAZ also revealed that these cells had increased Caspase-3 and -7 (3/7) activity (Fig. 4C), suggesting that these cells were undergoing increased apoptosis. Furthermore, knockdown of either YAP or TAZ decreased the ability of SCC2 cells to migrate in wound closure scratch assays, with knockdown of both YAP and TAZ almost completely halting cell migration (Fig. 4D).

We next examined whether induced nuclear YAP and TAZ activity could drive pro-tumorigenic behavior in non-metastatic CAL27 cells. For these studies, CAL27 cells were engineered to express, in a doxycycline-inducible manner, the nuclear-localized YAP-5SA mutant (S61A, S109A, S127A, S164A, S397A), or YAP-5SA/S94A, which has an additional mutation that disrupts binding to the TEAD transcription factors (4, 31) (Fig. 4E). In contrast to YAP/TAZ depletion in SCC2 cells, ectopic expression of YAP-5SA increased the ability of CAL27 cells to proliferate (Fig. 4F). YAP-induced proliferation relied on TEAD binding, as expression of the YAP-5SA/S94A mutant failed to increase proliferation (Fig. 4F). Expression of YAP-5SA, but not YAP-5SA/S94A, also reduced Caspase 3/7 activity in the CAL27 cells (Fig. 4G), suggesting that nuclear YAP-TEAD-driven transcription induces pro-survival signals. Moreover, YAP-5SA, but not YAP-5SA/S94A, increased the ability of CAL27 cells to migrate (Fig. 4H). Taken together, our observations indicate that nuclear YAP and TAZ promote the proliferation, survival, and migration of OSCC cell lines *in vitro*, and suggest that the increased nuclear YAP observed in OSCC is an important contributing factor to disease progression.

To test whether YAP and TAZ drive pro-tumorigenic properties in OSCC cells *in vivo*, we knocked down YAP or YAP/TAZ in SCC2 cells and used them in tongue orthotopic xenograft tumor experiments in immunocompromised mice. We used SCC2 cells since they exhibit high nuclear YAP levels and have metastatic potential (19). To easily track tumor development and metastasis, we generated SCC2 cells expressing dsRED (SCC2-dsRED) and then engineered them to express control shRNA (shCTL), shRNA targeting YAP (shYAP), or shRNA targeting both YAP and TAZ (shYAP/TAZ). We chose not to knock down TAZ alone in these experiments given the less robust effects observed in our *in vitro* experiments. Stable knockdown was confirmed in these cells by immunoblotting (Fig. 5A), and the cells were then injected into the tongue of mice (Fig. 5B). Primary tumor growth was monitored with caliper measurements and also by IVIS imaging to locate dsRED-expressing cells. We found that YAP or YAP/TAZ knockdown decreased primary tumor

volume, with YAP/TAZ suppressing tumor growth more dramatically (Fig. 5B and 5C). Imaging after 22 days revealed abundant SCC2 cell metastasis, which was reduced with YAP knockdown, and almost completely ablated with YAP/TAZ knockdown (Fig. 5C). Thus, our mouse experiments indicated that YAP and TAZ have important roles in OSCC tumor growth and metastasis, suggesting that dysregulated nuclear YAP in oral tissues is relevant for OSCC onset and progression.

YAP/TAZ promote a transcriptional program that is associated with human OSCC progression

Our *in vitro* and *in vivo* studies suggested that the transcriptional activity of YAP and TAZ influence pro-tumorigenic events in OSCC cells. We therefore set out to understand YAP/TAZ-regulated transcription by using microarrays to compare the global expression profiles of SCC2 cells transfected with either control siRNA, or siRNA targeting TAZ, YAP, or both YAP/TAZ. Hierarchical clustering of the top 3000 genes with the highest median absolute deviation (MAD) showed that the expression profiles from replicate samples clearly clustered next to each other. Notably, the expression profiles from the control cells and the TAZ-depleted cells clustered similarly, whereas those from cells depleted of YAP or YAP/TAZ had similar expression profiles (Fig. 6A). Thus, YAP appears to have more prominent transcriptional role in SCC2 cells compared to TAZ, which was supported by our functional experiments shown in Fig. 4. Next, we carried out differential analyses of the control siRNA-treated samples versus the knockdown samples. For each treatment, we identified the signatures of up- (*repressed*) and down-regulated (*activated*) genes with adjusted p-value ≤0.05 and fold-change ≥2. The number of genes included in each signature is summarized in Fig. 6A, and they are listed in Supplementary Table 4.

To gain insight into whether the YAP- and TAZ-regulated gene expression signatures relate to OSCC onset and/or progression we used the following two methods to make comparisons with gene expression data generated by TCGA: 1) we tested for gene enrichment in tumor grade or stage data using Gene Set Enrichment Analysis (GSEA); and 2) we used Adaptive Signature Selection and InteGratioN (ASSIGN) to capture the coordinated co-expression of YAP/TAZ targets reflecting the corresponding regulators' *activity*. Our GSEA analysis revealed a significant enrichment (nominal p-values ≤0.05) for genes activated by YAP or YAP/TAZ (i.e. decreasing in our microarrays with knockdown) when compared to genes with elevated expression in tumor versus adjacent epithelium (Fig. 6B and Supplementary Fig. S3A). Enrichment of the YAP- and YAP/TAZ-regulated gene expression signature was preserved with elevated tumor grade (Fig. 6B) and tumor stage (Fig. 6C), even when comparing aggressive stage IV OSCCs to earlier stages (Fig. 6C, Supplementary Fig. S3B), suggesting that in addition to events necessary for tumor onset, YAP/TAZ activities also control processes required for late stage OSCC progression. Similar data were obtained from our ASSIGN analyses, which showed a significant upward trend of the YAP/TAZ activity score as a function of an increasing tumor grade and stage (Supplementary Fig. S4A and S4B). Together these data indicate that a subset of genes dysregulated in human OSCCs is associated with aberrant YAP/TAZ-activity.

The YAP/TAZ-regulated gene expression signature included canonical YAP/TAZ targets, such as *CTGF* or *CYR61*. However, no significant change in the expression of these genes was observed with respect to tumor onset, tumor grade, or tumor stage (Supplementary Fig. S5A and S5B), suggesting that the roles of YAP/TAZ in OSCCs extend beyond what has been characterized in other contexts. To better understand the cues regulated by YAP/TAZ in OSCC we clustered our identified gene expression signature with TCGA-derived OSCC tumor grade and stage expression changes. Clustering uncovered clear segregation of adjacent epithelium (white marked columns in Fig. 6D) and tumor samples (green marked columns in Fig. 6D), and further revealed tumor-associated sub-clusters of YAP/TAZ-regulated genes, the most prominent of which correlated with genes induced in expression by YAP/TAZ (yellow cluster in Fig. 6D). A more focused cluster analysis of only these activated genes revealed two major sub-groups, which we termed Cluster A and Cluster B (Fig. 6E, outlined in Supplementary Table 5). Annotation of these gene clusters by pathway hyper-enrichment analysis yielded a strong enrichment of cell cycle-related pathways in Cluster A (listed in Supplementary Table 6), all of which showed increased expression with tumor grade or stage when examined in the TCGA datasets (Supplementary Fig. S5C and S5D). Cluster B showed enrichment for genes responding to signals mediated by AP1, Hippo, TGF-beta, and WNT pathways (listed in Supplementary Table 6). Notably, several transcription factors relevant to tumor progression were also altered in Cluster B, and included TEAD1, TEAD4, ETS1, JUN, PBX3, RUNX2 and SOX9.

To validate whether the genes identified in Clusters A and B were indeed regulated by YAP and TAZ, we examined the expression of subset of these genes by quantitative real-time PCR (qPCR) in SCC2 cells transfected with control siRNA, or siRNA targeting TAZ, YAP, or both YAP/TAZ, as well as in CAL27 cells that expressed (24 h of ectopic expression) the nuclear YAP-5SA mutant or the transcriptionally defective YAP-5SA-S94A mutant. We initially focused on genes critical for cell cycle progression (*CCNE2*, *CDK2*, *CDC6*, *PCNA*, *AURKA*, *PLK4*), and pro-survival (*BIRC5*), both of which were associated with Cluster A in Fig. 6B. We found that knockdown of YAP/TAZ in SCC2 cells strikingly reduced the expression of all cell cycle and survival genes found in Cluster A (Fig. 7A). YAP knockdown also repressed the expression of these genes, some of which mirrored YAP/TAZ knockdown, while others were less affected, suggesting that TAZ redundantly regulates the expression of some of these genes. TAZ knockdown alone, however, had minor effects on the expression of almost all of these genes, suggesting that YAP/TAZ redundancy may only be revealed upon YAP deficiency in these cells. These same cell cycle and pro-survival genes were significantly induced by YAP-5SA expression in CAL27 cells (Fig. 7B), but were not affected by the expression of the transcriptionally defective YAP-5SA/S94A mutant, suggesting that nuclear YAP-TEAD activity directly regulates the expression of these genes. The transcription factors identified in Cluster B were all down-regulated following YAP/TAZ and YAP knockdown in SCC2 cells (Fig. 7A). However, the expression of these genes was largely unaffected following YAP-5SA expression in CAL27 cells, suggesting that some of these genes may not be direct YAP targets, or that they require additional factors or signals present in more progressed OSCCs for YAP-directed regulation. Interestingly, the exception was the regulation of *TEAD1* and *TEAD4*, as the expression of both of these TEAD family members was increased by YAP-5SA, but not by the YAP-5SA/

S94A mutant, in CAL27 cells (Fig. 7B). Further, analysis of gene expression across tumor grade using TCGA data showed that *TEAD4* is induced in expression with tumor onset, and further increases with higher tumor grade and stage (Fig. 7C). *TEAD1* did not show the same trends (Supplementary Fig. S5E). Thus, our data suggest that *TEAD4* may function as a relevant YAP/TAZ target that initiates a pro-tumorigenic feed-forward cascade that contributes to the onset and progression OSCC.

Discussion

This study provides evidence that the transcriptional regulators YAP and TAZ have important roles in the onset and progression of human OSCC. Notably, we have found that YAP localization is dysregulated in regions predisposed to OSCC onset, as increased nuclear YAP accumulation can be detected in epithelial cells of hyperplastic and dysplastic tissues. Thus, altered YAP localization correlates with the early transformation of oral epithelial cells, suggesting that nuclear YAP promotes their progression to a malignant state. Indeed, knockdown of YAP in SCC2 cells inhibited the ability of these cells to proliferate *in vitro*, and reduced the ability of these cells to generate tongue tumors *in vivo*. YAP knockdown in CAL27 cells also inhibited cell proliferation and anchorage-independent growth (28). Moreover, ectopic expression of a nuclear-localized YAP mutant in CAL27 cells promoted cell proliferation, indicating that nuclear YAP is sufficient to drive cell proliferation. Ectopic expression of nuclear-localized YAP also increased the ability for CAL27 cells to promote wound closure *in vitro*, and while we cannot rule out that these differences do not relate to proliferative alterations, our observations suggest that nuclear YAP activity is also sufficient to drive cell migration. Due to technical issues we were unable to similarly examine the localization of TAZ in human tissues, but given that common regulatory signals control YAP and TAZ localization (8), and that TAZ plays an important role in other cancer cells (20, 32), it is likely that dysregulated TAZ localization also contributes to early OSCC development. Supporting this premise, we found that knockdown of both YAP and TAZ in SCC2 OSCC cells severely reduced their proliferation, induced pro-apoptotic cues, and halted their wound closure potential *in vitro*, beyond the knockdown of either YAP or TAZ alone. Additionally, knockdown of both YAP and TAZ dramatically reduced primary tumor growth *in vivo*, more so than YAP knockdown alone. Thus, YAP and TAZ have redundant pro-tumorigenic roles, which may be the case for other malignancies in addition to OSCC.

While our observations indicate accumulation of nuclear YAP in tissues predisposed to form OSCC, how this dysregulation arises is less clear. Interrogation of TCGA datasets showed no indication of general increases in *YAP* (or *TAZ*) expression or genomic alterations with OSCC onset, or altered expression of core Hippo pathway components known to regulated YAP/TAZ localization. Given the close association between epithelial cell polarity cues and the control of YAP localization (33, 34), and the observed epithelial polarity changes that occur with OSCC onset (35), one possibility is that altered epithelial polarity cues may contribute to the dysregulation of YAP. Another unresolved question relates to why only subsets of tumors exhibit abundant levels of YAP protein. Our analysis showed that four out of the ten tumors (ranging from moderately to poorly differentiated) that we examined had elevated YAP levels. While the increased YAP levels in these distinct tumors may result

from amplified expression of *YAP*, as suggested by prior studies (27, 29), they may also relate to alternative mechanisms of post-transcriptional control of YAP stability and localization. Phosphorylation of YAP on S127 was reduced in tumors with elevated YAP, suggesting that defective Hippo pathway signaling likely contributes to these aberrant YAP levels. Notably, the tumors we identified with high YAP levels were characterized as poorly differentiated, suggesting that YAP may contribute to tumor progression. High YAP levels with prominent nuclear localization were observed in the basal layer of adjacent histopathologically normal epithelia, which is similar to that observed in the basal progenitors of the epidermis (33), proximal lung epithelium (36, 37), and a range of other epithelial stem cell populations throughout development (8). Thus, nuclear YAP activity may facilitate the oral epithelial progenitor state and possibly contribute to stem cell-like properties observed in aggressive OSCCs.

The pro-tumorigenic activity of YAP and TAZ rely on their transcriptional properties (4, 38). Using global gene expression analysis following the knockdown of YAP/TAZ in OSCC cells we have identified a transcriptional program that is regulated by these factors. This YAP/TAZ expression signature correlates with gene expression changes identified by TCGA in OSCC, indicating that YAP/TAZ is broadly dysregulated with OSCC onset. Strikingly, genes induced in expression by YAP/TAZ (i.e. genes repressed following YAP/TAZ knockdown) are significantly associated with OSCC progression, as the expression changes are maintained with advancing tumor grade and tumor stage. This includes stage IV tumors, which have the lowest 5-year survival rates (39). Our data showing that YAP/TAZ may promote OSCC cell migration and progression to a metastatic state in mouse orthotopic tongue tumor models suggest that YAP/TAZ participate in pro-metastatic events in OSCC, as is the case in other malignancies (32, 38), but further work is required to clarify this possibility.

Hierarchical clustering analysis of the YAP/TAZ-induced genes with OSCC tumor grade and stage progression revealed two clusters that suggest YAP/TAZ function in OSCC. One of these clusters (Cluster A in our Fig. 6) was enriched for genes critical for cell cycle progression, and likely explains the pro-proliferation roles that YAP/TAZ play in OSCC cells. Genes regulated by the ATR- and E2F- transcription factors are enriched in this cluster, suggesting that YAP/TAZ may direct the activity of these transcription factors to overcome cell cycle checkpoints. The second cluster (Cluster B in our Fig. 6) was enriched for genes that respond to cancer-related signaling pathways, such as those regulated by TGF-beta and Wnt growth factors. Nuclear YAP and/or TAZ synergize with TGF-beta-activated Smad transcription factors to promote pro-tumorigenic events (40, 41), and thus, it is likely that nuclear YAP/TAZ promote these signals in OSCC. Similarly, nuclear YAP/TAZ facilitate Wnt-induced signals (42, 43), which have key roles in the development of OSCC (22). Wnt and TGF-beta signaling both promote epithelial-mesenchymal transition (EMT), which is a process implicated in the induction of tumor-initiating properties (44). EMT-related genes were enriched in the YAP/TAZ-regulated transcriptional signature, as were gene targets of the stem cell-regulating transcription factor OCT4. Thus, the YAP/TAZ-induced transcriptional program may influence tumor-initiating properties that are associated with aggressive OSCC. Additional transcription factors implicated in cancer

progression were also regulated by YAP/TAZ, including SOX9, which has recently been described as a target of YAP in esophageal cancers (45). Notably, members of the TEAD family were induced by YAP/TAZ, and increased expression of *TEAD4* was significantly elevated with increased OSCC grade and stage. Thus, early increases in nuclear YAP/TAZ localization may initiate a feed-forward mechanism that promotes the assembly of YAP/TAZ-TEAD complexes. Given that binding to TEAD transcription factors drives YAP/TAZ nuclear accumulation (46), such a feed-forward mechanism may contribute to the elevated nuclear YAP/TAZ observed with OSCC development.

Taken together our observations indicate that YAP/TAZ are important factors contributing to OSCC biology. Our data highlight the importance of examining changes beyond single gene expression, mutation, and/or genomic alterations that correlate with cancer tissues, as our focused analysis of the YAP/TAZ-regulated signature identifies and connects tumor-associated expression changes that may be otherwise overlooked. Given that YAP/TAZ are dysregulated early in the onset of OSCC, further understanding the YAP/TAZ-regulated transcriptional events and linking them to other cancer-related signaling networks may offer new insight into OSCC. Moreover, given the emergence of small molecules that target YAP/TAZ activity, novel therapeutic approaches may evolve that can hopefully reduce this devastating disease.

Supplementary Material

Refer to Web version on PubMed Central for supplementary material.

Acknowledgments

We thank the Boston University Oral Cancer Research Initiative (OCRI) and the Oral Cancer Affinity Research Collaborative group at Boston University for funds to perform the microarray analysis, as well as Adam Gower and the Boston University Microarray Core for help with microarray data analysis (CTSI grant #U54-TR001012). XV is funded by Research Grant No. 1-FY14-219 from the March of Dimes Foundation, by the CDMRP (W81XWH-14-1-0336), and by the NIH-National Heart Lung and Blood Institute (1R01HL124392-01). MK was funded by the NIH-National Institute of Dental and Craniofacial Research (DE RO1 014437). LZ and SM were funded in part by a Massachusetts Green High-Performance Computing Center grant.

References

1. Varelas X, Kukuruzinska MA. Head and neck cancer: from research to therapy and cure. Annals of the New York Academy of Sciences. 2014; 1333:1–32. [PubMed: 25532687]
2. Harvey KF, Zhang X, Thomas DM. The Hippo pathway and human cancer. Nat Rev Cancer. 2013; 13:246–57. [PubMed: 23467301]
3. Vassilev A, Kaneko KJ, Shu H, Zhao Y, DePamphilis ML. TEAD/TEF transcription factors utilize the activation domain of YAP65, a Src/Yes-associated protein localized in the cytoplasm. Genes & development. 2001; 15:1229–41. [PubMed: 11358867]
4. Zhao B, Ye X, Yu J, Li L, Li W, Li S, et al. TEAD mediates YAP-dependent gene induction and growth control. Genes & development. 2008; 22:1962–71. [PubMed: 18579750]
5. Camargo FD, Gokhale S, Johnnidis JB, Fu D, Bell GW, Jaenisch R, et al. YAP1 increases organ size and expands undifferentiated progenitor cells. Curr Biol. 2007; 17:2054–60. [PubMed: 17980593]
6. Chan SW, Lim CJ, Guo K, Ng CP, Lee I, Hunziker W, et al. A role for TAZ in migration, invasion, and tumorigenesis of breast cancer cells. Cancer Res. 2008; 68:2592–8. [PubMed: 18413727]

7. Dong J, Feldmann G, Huang J, Wu S, Zhang N, Comerford SA, et al. Elucidation of a universal size-control mechanism in Drosophila and mammals. Cell. 2007; 130:1120–33. [PubMed: 17889654]
8. Varelas X. The Hippo pathway effectors TAZ and YAP in development, homeostasis and disease. Development. 2014; 141:1614–26. [PubMed: 24715453]
9. Kanai F, Marignani PA, Sarbassova D, Yagi R, Hall RA, Donowitz M, et al. TAZ: a novel transcriptional co-activator regulated by interactions with 14–3-3 and PDZ domain proteins. Embo J. 2000; 19:6778–91. [PubMed: 11118213]
10. Zhao B, Li L, Tumaneng K, Wang CY, Guan KL. A coordinated phosphorylation by Lats and CK1 regulates YAP stability through SCF(beta-TRCP). Genes & development. 2010; 24:72–85. [PubMed: 20048001]
11. Piccolo S, Dupont S, Cordenonsi M. The biology of YAP/TAZ: hippo signaling and beyond. Physiological reviews. 2014; 94:1287–312. [PubMed: 25287865]
12. Ramos A, Camargo FD. The Hippo signaling pathway and stem cell biology. Trends Cell Biol. 2012; 22:339–46. [PubMed: 22658639]
13. Muramatsu T, Imoto I, Matsui T, Kozaki K, Haruki S, Sudol M, et al. YAP is a candidate oncogene for esophageal squamous cell carcinoma. Carcinogenesis. 2011; 32:389–98. [PubMed: 21112960]
14. Wei Z, Wang Y, Li Z, Yuan C, Zhang W, Wang D, et al. Overexpression of Hippo pathway effector TAZ in tongue squamous cell carcinoma: correlation with clinicopathological features and patients' prognosis. Journal of oral pathology & medicine: official publication of the International Association of Oral Pathologists and the American Academy of Oral Pathology. 2013; 42:747–54.
15. Ge L, Smail M, Meng W, Shyr Y, Ye F, Fan KH, et al. Yes-associated protein expression in head and neck squamous cell carcinoma nodal metastasis. PLoS One. 2011; 6:e27529. [PubMed: 22096589]
16. Hall CA, Wang R, Miao J, Oliva E, Shen X, Wheeler T, et al. Hippo pathway effector Yap is an ovarian cancer oncogene. Cancer Res. 2010; 70:8517–25. [PubMed: 20947521]
17. Jerhammar F, Johansson AC, Ceder R, Welander J, Jansson A, Grafstrom RC, et al. YAP1 is a potential biomarker for cetuximab resistance in head and neck cancer. Oral oncology. 2014; 50:832–9. [PubMed: 24993889]
18. Schmitz S, Ang KK, Vermorken J, Haddad R, Suarez C, Wolf GT, et al. Targeted therapies for squamous cell carcinoma of the head and neck: current knowledge and future directions. Cancer treatment reviews. 2014; 40:390–404. [PubMed: 24176789]
19. Patel V, Marsh CA, Dorsam RT, Mikelis CM, Masedunskas A, Amornphimoltham P, et al. Decreased lymphangiogenesis and lymph node metastasis by mTOR inhibition in head and neck cancer. Cancer Res. 2011; 71:7103–12. [PubMed: 21975930]
20. Hiemer SE, Szymaniak AD, Varelas X. The transcriptional regulators TAZ and YAP direct transforming growth factor beta-induced tumorigenic phenotypes in breast cancer cells. The Journal of biological chemistry. 2014; 289:13461–74. [PubMed: 24648515]
21. Stewart SA, Dykxhoorn DM, Palliser D, Mizuno H, Yu EY, An DS, et al. Lentivirus-delivered stable gene silencing by RNAi in primary cells. Rna. 2003; 9:493–501. [PubMed: 12649500]
22. Jamal B, Sengupta PK, Gao ZN, Nita-Lazar M, Amin B, Jalisi S, et al. Aberrant amplification of the crosstalk between canonical Wnt signaling and N-glycosylation gene DPAGT1 promotes oral cancer. Oral oncology. 2012; 48:523–9. [PubMed: 22341307]
23. Irizarry RA, Hobbs B, Collin F, Beazer-Barclay YD, Antonellis KJ, Scherf U, et al. Exploration, normalization, and summaries of high density oligonucleotide array probe level data. Biostatistics. 2003; 4:249–64. [PubMed: 12925520]
24. Dai M, Wang P, Boyd AD, Kostov G, Athey B, Jones EG, et al. Evolving gene/transcript definitions significantly alter the interpretation of GeneChip data. Nucleic Acids Res. 2005; 33:e175. [PubMed: 16284200]
25. Liberzon A, Subramanian A, Pinchback R, Thorvaldsdottir H, Tamayo P, Mesirov JP. Molecular signatures database (MSigDB) 3.0. Bioinformatics. 2011; 27:1739–40. [PubMed: 21546393]

26. Subramanian A, Tamayo P, Mootha VK, Mukherjee S, Ebert BL, Gillette MA, et al. Gene set enrichment analysis: a knowledge-based approach for interpreting genome-wide expression profiles. Proc Natl Acad Sci U S A. 2005; 102:15545–50. [PubMed: 16199517]
27. Ehsanian R, Brown M, Lu H, Yang XP, Pattatheyil A, Yan B, et al. YAP dysregulation by phosphorylation or DeltaNp63-mediated gene repression promotes proliferation, survival and migration in head and neck cancer subsets. Oncogene. 2010; 29:6160–71. [PubMed: 20729916]
28. Zhang L, Ye DX, Pan HY, Wei KJ, Wang LZ, Wang XD, et al. Yes-associated protein promotes cell proliferation by activating Fos Related Activator-1 in oral squamous cell carcinoma. Oral oncology. 2011; 47:693–7. [PubMed: 21708480]
29. Dong G, Loukinova E, Chen Z, Gangi L, Chanturita TI, Liu ET, et al. Molecular profiling of transformed and metastatic murine squamous carcinoma cells by differential display and cDNA microarray reveals altered expression of multiple genes related to growth, apoptosis, angiogenesis, and the NF-kappaB signal pathway. Cancer Res. 2001; 61:4797–808. [PubMed: 11406555]
30. Basu S, Totty NF, Irwin MS, Sudol M, Downward J. Akt phosphorylates the Yes-associated protein, YAP, to induce interaction with 14–3-3 and attenuation of p73-mediated apoptosis. Mol Cell. 2003; 11:11–23. [PubMed: 12535517]
31. Zhao B, Wei X, Li W, Udan RS, Yang Q, Kim J, et al. Inactivation of YAP oncoprotein by the Hippo pathway is involved in cell contact inhibition and tissue growth control. Genes & development. 2007; 21:2747–61. [PubMed: 17974916]
32. Cordenonsi M, Zanconato F, Azzolin L, Forcato M, Rosato A, Frasson C, et al. The Hippo Transducer TAZ Confers Cancer Stem Cell-Related Traits on Breast Cancer Cells. Cell. 2011; 147:759–72. [PubMed: 22078877]
33. Schlegelmilch K, Mohseni M, Kirak O, Pruszak J, Rodriguez JR, Zhou D, et al. Yap1 acts downstream of alpha-catenin to control epidermal proliferation. Cell. 2011; 144:782–95. [PubMed: 21376238]
34. Varelas X, Samavarchi-Tehrani P, Narimatsu M, Weiss A, Cockburn K, Larsen BG, et al. The Crumbs complex couples cell density sensing to Hippo-dependent control of the TGF-beta-SMAD pathway. Developmental cell. 2010; 19:831–44. [PubMed: 21145499]
35. Nita-Lazar M, Noonan V, Rebustini I, Walker J, Menko AS, Kukuruzinska MA. Overexpression of DPAGT1 leads to aberrant N-glycosylation of E-cadherin and cellular discohesion in oral cancer. Cancer Res. 2009; 69:5673–80. [PubMed: 19549906]
36. Mahoney JE, Mori M, Szymaniak AD, Varelas X, Cardoso WV. The hippo pathway effector Yap controls patterning and differentiation of airway epithelial progenitors. Developmental cell. 2014; 30:137–50. [PubMed: 25043473]
37. Zhao R, Fallon TR, Saladi SV, Pardo-Saganta A, Villoria J, Mou H, et al. Yap tunes airway epithelial size and architecture by regulating the identity, maintenance, and self-renewal of stem cells. Developmental cell. 2014; 30:151–65. [PubMed: 25043474]
38. Lamar JM, Stern P, Liu H, Schindler JW, Jiang ZG, Hynes RO. The Hippo pathway target, YAP, promotes metastasis through its TEAD-interaction domain. Proc Natl Acad Sci U S A. 2012; 109:E2441–50. [PubMed: 22891335]
39. Chen GS, Chen CH. A study on survival rates of oral squamous cell carcinoma. The Kaohsiung journal of medical sciences. 1996; 12:317–25. [PubMed: 8699569]
40. Hiemer SE, Varelas X. Stem cell regulation by the Hippo pathway. Biochim Biophys Acta. 2013; 1830:2323–34. [PubMed: 22824335]
41. Varelas X, Sakuma R, Samavarchi-Tehrani P, Peerani R, Rao BM, Dembowy J, et al. TAZ controls Smad nucleocytoplasmic shuttling and regulates human embryonic stem-cell self-renewal. Nat Cell Biol. 2008; 10:837–48. [PubMed: 18568018]
42. Azzolin L, Panciera T, Soligo S, Enzo E, Bicciato S, Dupont S, et al. YAP/TAZ incorporation in the beta-catenin destruction complex orchestrates the Wnt response. Cell. 2014; 158:157–70. [PubMed: 24976009]
43. Varelas X, Miller BW, Sopko R, Song S, Gregorieff A, Fellouse FA, et al. The Hippo pathway regulates Wnt/beta-catenin signaling. Developmental cell. 2010; 18:579–91. [PubMed: 20412773]

44. Mani SA, Guo W, Liao MJ, Eaton EN, Ayyanan A, Zhou AY, et al. The epithelial-mesenchymal transition generates cells with properties of stem cells. Cell. 2008; 133:704–15. [PubMed: 18485877]

45. Song S, Ajani JA, Honjo S, Maru DM, Chen Q, Scott AW, et al. Hippo Coactivator YAP1 Upregulates SOX9 and Endows Esophageal Cancer Cells with Stem-like Properties. Cancer Res. 2014; 74:4170–82. [PubMed: 24906622]

46. Chan SW, Lim CJ, Loo LS, Chong YF, Huang C, Hong W. TEADs mediate nuclear retention of TAZ to promote oncogenic transformation. The Journal of biological chemistry. 2009; 284:14347–58. [PubMed: 19324876]

Implications

This study defines a YAP/TAZ-regulated transcriptional program in OSCC, and reveals novel roles for nuclear YAP/TAZ activity in the onset and progression of this cancer.

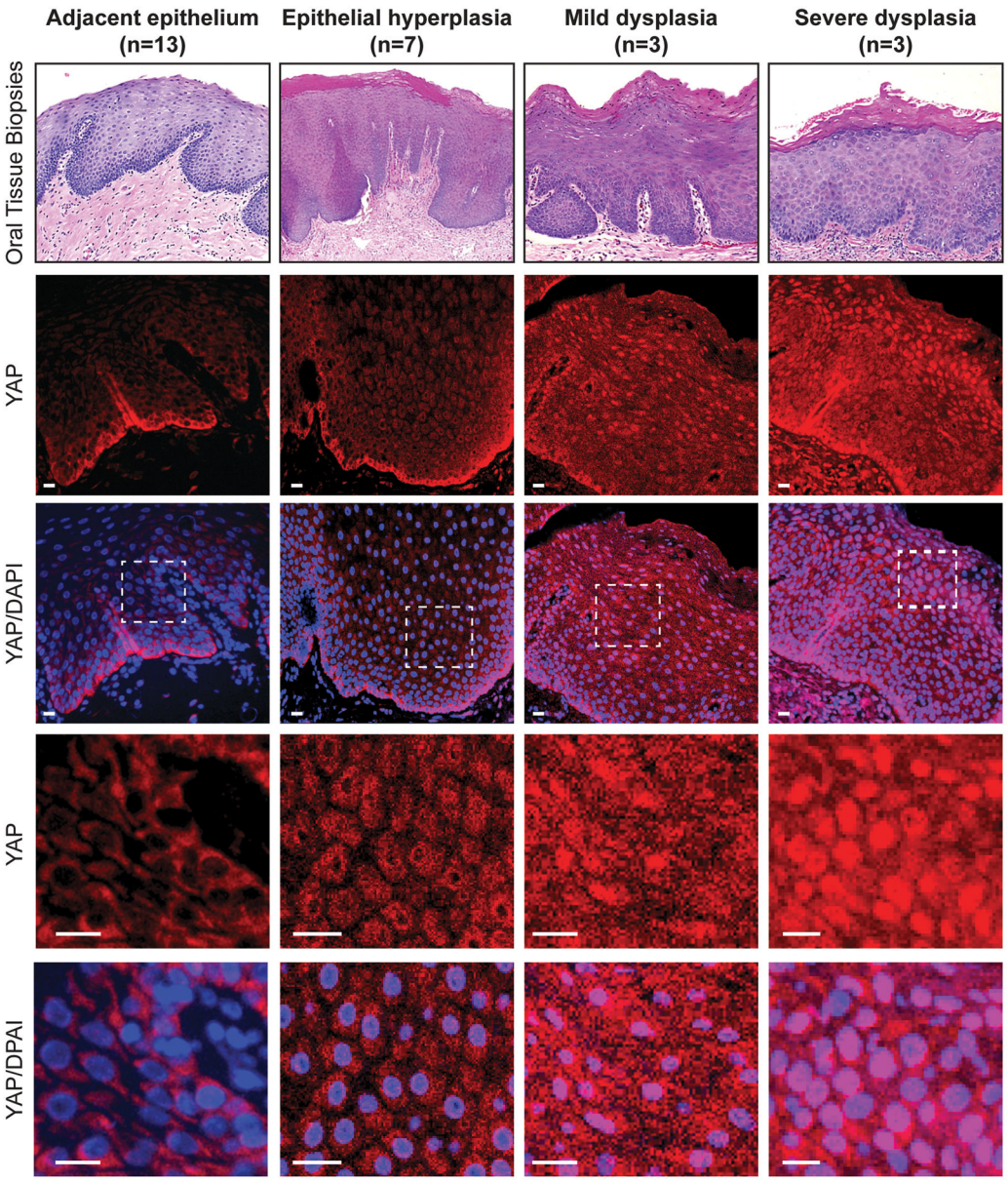

Figure 1.

Nuclear YAP accumulates in oral tissues with hyperplasia and dysplasia pathology. Tissues from patients exhibiting hyperplasia, mild dysplasia and severe dysplasia, as well as cytologically normal adjacent epithelium, were examined by H&E staining (top panels) and by immunofluorescence to detect YAP localization (the number of tissues examined is indicated). DAPI was used to stain nuclei. A zoomed in image from each sample is shown in the bottom panels, highlighting the YAP localization changes observed. Scale bars represent 20μm.

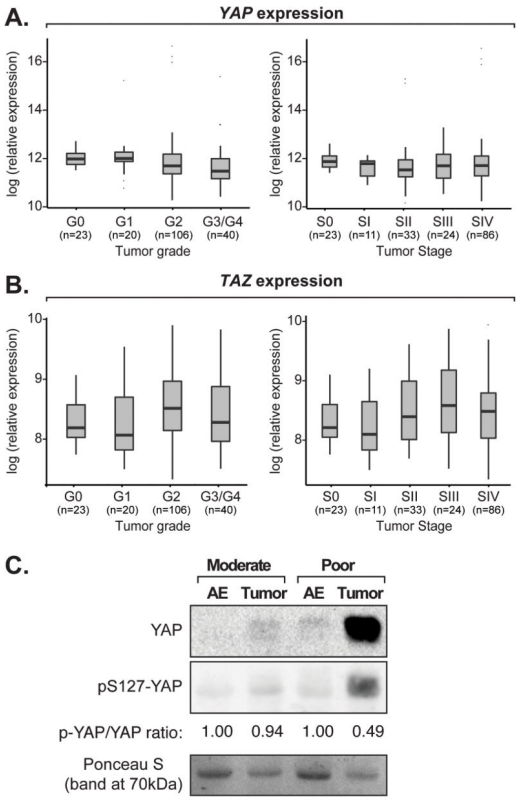

Figure 2.

YAP and *TAZ* expression in OSCCs. One-way ANOVA analysis showing **(A)** *YAP* or **(B)** *TAZ* expression with respect to TCGA OSCC tumor grade or stage data. A pairwise t-test analysis comparing datasets revealed no significant expression changes. **(C**) Protein was extracted from poorly and moderately differentiated tumors, and associated adjacent epithelium (AE), and examined for YAP and pS127-YAP levels by immunoblotting. A representative image of our results is shown. Ponceau-S staining of the proteins on the immunoblotted membrane is shown as a loading control. Quantitation of the relative phospho-S127-YAP to total YAP is also shown.

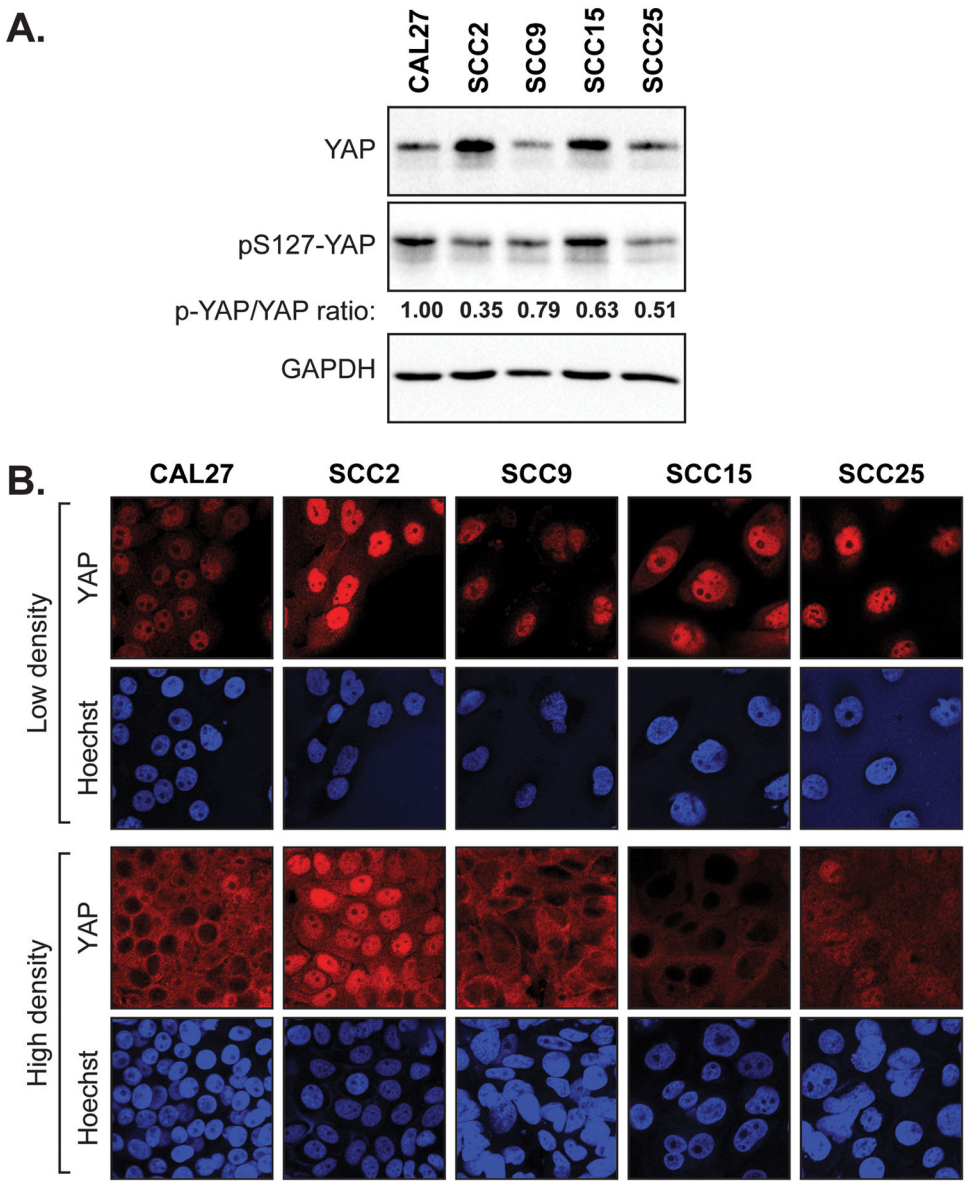

Figure 3.

Elevated levels of nuclear YAP are found in aggressive OSCC cells. **(A)** A panel of oral cancer cell lines was examined by immunoblotting for endogenous YAP, phospho-S127-YAP, and GAPDH (loading control). Quantification of phospho-S127-YAP to total YAP is shown. **(B)** Oral cancer cell lines were examined by immunofluorescence for endogenous YAP localization at both low and high density.

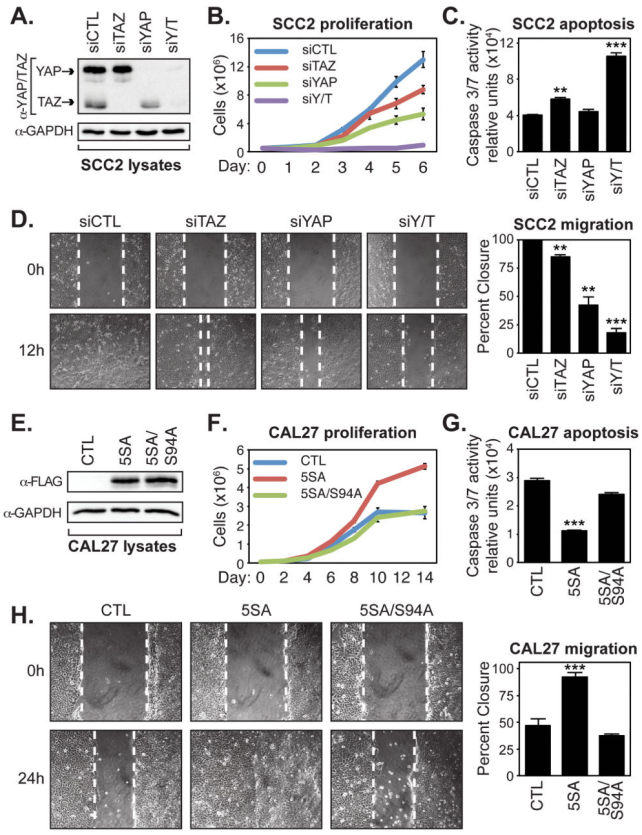

Figure 4.

YAP/TAZ promote OSCC cell proliferation, survival, and migration. **(A)** SCC2 cells were transfected with control siRNA (siCTL) or siRNA targeting TAZ (siTAZ), YAP (siYAP), or YAP and TAZ (siYAP/TAZ), and lysates obtained from these cells were examined by immunoblotting with the indicated antibodies. (**B**) SCC2 knockdown cells were counted over 6 days to measure their proliferative capacity. Cells from three experiments were counted and the average (+S.E.) for each day is shown. (**C**) SCC2 knockdown cells were examined for Caspase-3 and -7 activity using a Caspase-Glo 3/7 assay. The average (+S.E.) of three experiments is shown. (**D**) Confluent monolayers of SCC2 knockdown cells were wounded and examined for their ability to migrate after 12 hours. Representative images are shown and the average wound healing (+S.E.) of three experiments is indicated. (**E**) Doxycycline-inducible CAL27 control cells, or cells expressing 3xFLAG-YAP(5SA) or 3xFLAG-YAP(5SA/S94A) were lysed and examined by immunoblotting with the indicated antibodies. **(F)** CAL27 expressing cells were counted over 14 days to measure their proliferative capacity. Cells from three experiments were counted and the average (+S.E.) for each day is shown. (**G**) CAL27 expressing cells were examined for caspase-3 and -7 activity using a Caspase-Glo 3/7 assay. The average (+S.E.) of three experiments is shown. (**H**) Confluent monolayers of CAL27 expressing cells were wounded and examined for their ability to migrate after 24 hours. Representative images are shown and the average wound healing (+S.E.) of three experiments is indicated. All statistics were calculated compared to the control sample using an unpaired Student's *t* test and are represented as ** p-value<0.01, and *** p-value<0.001.

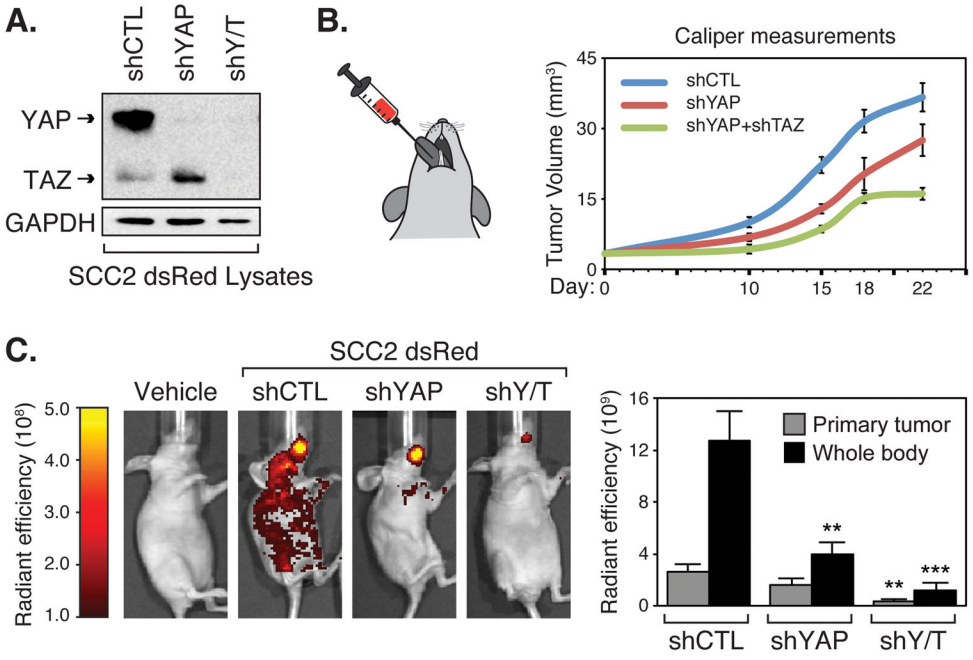

Figure 5.

YAP/TAZ are required for OSCC tumor growth and metastasis *in vivo*. **(A)** SCC2-dsRED cells stably expressing control shRNA (shCTL), shRNA targeting YAP (shYAP), or shRNA targeting YAP and TAZ (shY/T) were lysed and examined by immunoblotting for the indicated proteins. **(B)** SCC2-dsRED cells were injected into the tongue of nude mice and primary tumor volume was determined by caliper measurements at day 10, 15, 18, and 22. **(C)** SCC2-dsRED cells contributing to tumor formation and metastasis were visualized by IVIS fluorescent imaging at day 22 and representative images are shown. Total radiant efficiency of cells in the primary tumor and cells that metastasized throughout the animal body were quantitated and are shown as the average (+S.E.) (n=3 for vehicle control, n=9 for shRNA-expressing cells). Statistics comparing primary tumor size or metastasis of the knockdown cells to the control cells were performed using an unpaired Student's *t* test and are represented as ** p-value<0.01, and *** p-value<0.001.

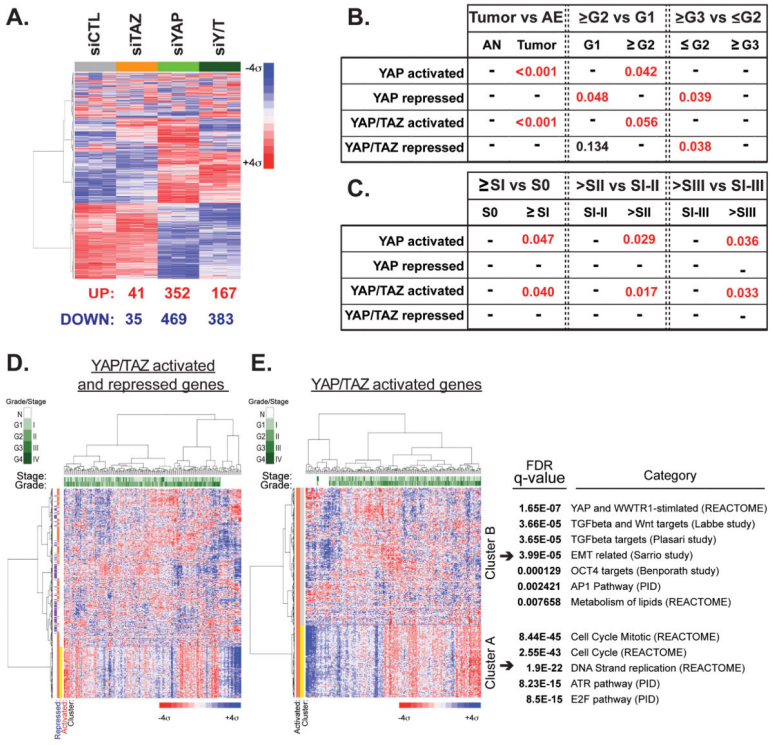

Figure 6.

YAP/TAZ-regulated transcriptional events correlate with OSCC tumor grade and stage. **(A)** Microarrays were performed from samples isolated from SCC2 cells transiently transfected with control siRNA (siCTL) or siRNA targeting TAZ (siTAZ), YAP (siYAP), or YAP and TAZ (siYAP/TAZ). Hierarchical clustering of the top 3000 genes with the highest median absolute deviation is shown. The number of up- and down-regulated genes (genes with adjusted p-value ≤0.05 and fold-change ≥2 compared to the control) that were identified from our microarray study is shown below. We tested for the enrichment of the YAP- and TAZ-regulated expression changes in the TCGA data by GSEA. The results for our analysis of **(B)** adjacent epithelium (AE) versus tumor grade and **(C)** tumor stages are summarized (enrichment nominal p-values reported). OSCC tumor grade and tumor stage data obtained from TCGA was projected onto **(D)** the entire YAP/TAZ-regulated expression signature identified from our microarray studies, or **(E)** only the YAP/TAZ-activated expression signature, and a heat map of the clustered data is shown. Two notable YAP/TAZ-activated gene clusters were identified, and selected data from our pathway enrichment analysis of these genes are shown on the right.

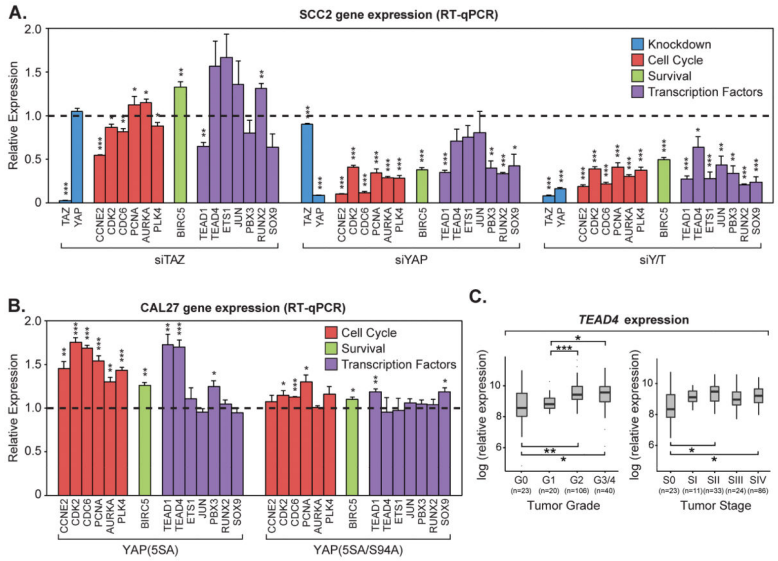

Figure 7.

YAP/TAZ regulate the transcription of genes important for cell cycle progression and survival. **(A)** SCC2 cells were transiently transfected with control siRNA (siCTL) or siRNA targeting TAZ (siTAZ), YAP (siYAP), or YAP and TAZ (siYAP/TAZ). Relative expression of genes indicated in the microarray analysis was determined by qPCR. All data are relative to siCTL (dashed line) and are shown as the average of three experiments (+S.E.). Genes are grouped together by function including knockdown efficiency (blue), cell cycle regulation (red), pro-survival (green), and transcription factors (purple). **(B)** Doxycycline-inducible CAL27 control cells or cells expressing 3xFLAG-YAP(5SA) or 3xFLAG-YAP(5SA/S94A) were treated with doxycycline. Relative expression of genes indicated in the microarray analysis was determined by qPCR. All data are relative to control cells (dashed line) and are shown as the average of three experiments (+S.E.). Genes are grouped together by function including cell cycle regulation (red), pro-survival (green), and transcription factors (purple). Statistics comparing to the control cells (dashed line) were calculated using an unpaired Student's *t* test and are represented as * p-value<0.05, ** p-value<0.01, and *** p-value<0.001. **(C)** Box plot of *TEAD4* expression with respect to OSCC tumor grade and stage, showing *TEAD4* expression is significantly induced with OSCC tumor grade (One-way ANOVA; p-value=3.51 e-05) and stage (One-way ANOVA; p-value=0.0012). Pairwise t-tests of expression between groups is also shown, and represented as * p-value<0.05, ** p-value<0.01, and *** p-value<0.001.